# QUANTUM EFFECTS ON THE CALORIC CURVES OF LITHIUM CLUSTERS

Fernand SPIEGELMAN[1,*] and Florent CALVO[2]

*Laboratoire de Chimie et Physique Quantiques, UMR5626 du CNRS, IRSAMC, Université Paul Sabatier, 118 Route de Narbonne, F-31062 Toulouse Cedex, France; e-mail: [1] fernand.spiegelman@irsamc.ups-tlse.fr, [2] florent.calvo@irsamc.ups-tlse.fr*

Received October 20, 2006
Accepted February 12, 2007

*Experience in many different areas of theoretical chemistry made Professor Jaroslav Koutecký a person with a broad interest, a wide and profound view, and highly open-minded. This was extremely valuable in an environment gathering researchers coming from various fields, not only chemistry, but also solid-state, molecular, and nuclear physics. One of us (F. Spiegelman) is particularly grateful to him for extended discussions during one of the early summer schools on elemental clusters in Erice in 1988, when F. S. was only starting in the field of cluster physics. This school took place at a moment where the confrontation between the jellium model and explicit Born–Oppenheimer calculations was the opportunity for many interesting discussions among theoreticians. The multiple roles of geometrical structure in metal clusters have been widely documented for a large part thanks to the contributions of J. Koutecký and his group. The present paper is dedicated to him.*

A tight-binding quantum Hamiltonian and an empirical embedded-atom model (EAM) potential are used to get insight into the finite-temperature behavior of small $Li_n$ clusters, $n$ = 8, 20, and 55. Exchange Monte Carlo simulations provide an extensive sampling of configuration space, including the putative global minimum and many relevant isomers. The heat capacities obtained from the classical simulations are corrected for low-temperature quantum delocalization using the Pitzer–Gwinn approximation. Alternatively, the caloric curves are estimated from the database of local minima using the quantum harmonic superposition approximation. While the two atomistic models predict qualitatively similar features, including some premelting effects in $Li_{20}$ but none in $Li_{55}$, strong variations are observed in the melting temperatures, the EAM potential giving unexpectedly low values.

**Keywords**: Caloric curves; Lithium clusters; Tight-binding; Embedded atom model; Monte Carlo simulations; Heat capacity.

Since the first experimental evidence of magic numbers in sodium clusters by Knight et al.[1], alkali clusters have been considered as representative prototypes of elemental atomic metal clusters. The first studies were aimed at understanding the onset of metallic character from an atom-per-atom growth perspective, but also the specificities of finite clusters, especially quantum



doi:10.1135/cccc20070278

size effects. In a first approximation, the magic numbers of simple metal clusters can be readily explained by the basic spherical jellium model[1,2], which assigns the special stabilities in terms of electronic shell closures, in analogy with the nuclear shell model or with atomic physics, thus reflecting some common trends with fermionic systems.

The jellium model[2] has been very fruitful in rationalizing trends in the electronic structure of simple metal clusters, mainly alkali and noble metal clusters, but also trivalent metal clusters. This model was also the basis for describing supershells, as early predicted for large finite fermionic systems. Supershells could not be observed in the case of nuclei due to their limited size, but they were actually evidenced in atomic clusters[3].

Even though several extensions of the jellium model have been developed[4], notably to cope with deformations, it has quickly become clear that clusters are not entirely similar to nuclei, and that their internal structure (the ions) do play a significant role. Obviously, accounting for the discrete ionic structure is important when trying to calculate properties quantitatively. A great merit of the group directed by J. Koutecký, and later by V. Bonačić-Koutecký, was to initiate and tackle this problem in small alkali metal clusters, using the *first principle* methods of quantum chemistry. In developing this area, J. Koutecký certainly benefited from his previous experience and achievements in various fields of theoretical chemistry, including the electronic many-body problem, semiempirical methods, electrochemistry, catalysis and reactivity. J. Koutecký and his group were thus able to elucidate the interplay between electronic and structural properties. This turned out to be of crucial importance, firstly to get intrinsic fundamental insight, and secondly because electronic properties can be directly observed in experiments (via spectroscopic measurements) while structure itself can only be inferred indirectly, by comparison with dedicated calculations. Only recently, the advent of infrared spectroscopy provided a closer access to the structure of small clusters formed in gas phase. In this respect, the contributions of J. Koutecký have laid the ground for development of realistic *ab initio* quantum chemistry studies of cluster spectroscopy and dynamics. Such studies have been of great impact for the interpretation and rationalization of detailed experimental observations, covering topics such as stability, fragmentation, geometry, and size evolution. Important contributions were also made in Jahn–Teller instabilities, excited states and optical spectra, the influence of charge, and more recently chemical reactivity. Feature articles reviewing important contributions of J. Koutecký in the field can be found for instance in refs[5–10].

The account of cluster geometry is clearly important for describing near-equilibrium properties, but it is also unavoidable as soon as dynamics or thermodynamics of clusters are concerned. Clusters exhibit structural, electronic, and thermodynamical properties which deviate significantly from the bulk behavior. These variations are often quantitative as in the lower binding energies or melting point generally observed in finite size systems, but can sometimes be more qualitative. For instance, bonding in mercury[11], gallium[12] or tin[13] clusters is found to be of van der Waals, covalent or metallic character, depending on the number of atoms. Lithium is the lightest species among simple metals. Experimentally, lithium clusters have been studied by mass spectrometry to measure their ionization potentials[14], polarizabilities[15] and their oscillators strength[16]. They have also been recently investigated by Raman spectroscopy[17]. Theoretically, and following the seminal *ab initio* study at the configuration interaction level by the Koutecký group[18], lithium clusters have been devoted contributions by many groups[17,19–41,43–46]. Beyond the jellium picture[26], several papers have emphasized complex spin states and magnetism[33,37,40,41,44] or unusual geometric structures[21,24]. The nature of chemical bonding was addressed using the electron localization function methodology[36], and resonating valence bond calculations have been reported as well[29,32]. The isomerization dynamics of selected cluster sizes has been investigated by the group of Koutecký and Bonačić-Koutecký[22,23,27] at the Hartree–Fock and density-functional theory levels, within the classical molecular dynamics framework. A similar Monte Carlo simulation was performed by Srinivas and Jellinek[35]. The fluxional character of the dynamics of lithium clusters is magnified by the zero-point motion, as studied in great details by Rousseau and Marx[30,31]. Using *ab initio* path integrals and Car–Parrinello dynamics, these authors showed that the static structures were destroyed by quantum delocalization, and that the multiple bond lengths were no longer seen at temperatures as low as 10 K [30,31]. More recently, Lee et al.[42] determined the caloric curves of $Li_{10}$ and $Li_{12}$ using *ab initio* DFT/LDA molecular dynamics, evidencing premelting features at low temperatures (a peak around 175 K for $Li_{10}$, a shoulder at 125 K for $Li_{12}$) and main maxima around 500–550 K.

As far as we are aware, no results are available on the finite-temperature behavior of lithium clusters containing more than 20 atoms. This situation contrasts with the case of sodium, for which a wealth of experimental[47] and theoretical[48–52] papers exist. In particular, the unexpected variations in the melting point of $Na_n^+$ clusters[47] seem to have been finally reproduced and interpreted[52].

At the present time, atomistic simulations at the *ab initio* path integrals level are currently not practical for sizes above 20 atoms, or aiming at sampling the disordered state. Fortunately, there are ways other than path integrals to incorporate quantum delocalization effects in thermodynamics. A first treatment consists in correcting the classical partition function at low temperatures by a quantum factor based on harmonic oscillators. This approximation, originally described by Pitzer and Gwinn[53], only requires knowledge of the vibrational frequencies of the lowest energy structure. It is also possible to construct the entire partition function itself by partitioning the configuration space into various basins of attraction corresponding to different isomers, summing their contributions at the harmonic[54] or higher[55] levels. For clusters that are too large to allow for a complete enumeration of isomers, reweighting[54] or dedicated sampling schemes[56] are required.

In this contribution, we use the two aforementioned approaches to calculate the caloric curves of several lithium clusters, incorporating vibrational delocalization effects. As in our previous work on sodium clusters[48,49,57] we employ two models for the potential energy surfaces (PES) of these clusters, namely a distance-dependent quantum tight-binding (TB) Hamiltonian and a simpler, explicit atomistic potential of the embedded-atom model (EAM) type. We also use recently developed sampling methods that allow an efficient search for the stable isomers, as well as a straightforward calculation of the classical caloric curves.

The paper is organized as follows. In the next section, the models and methods are summarized. In section "Application to Selected Lithium Clusters", the structures of $Li_8$, $Li_{20}$ and $Li_{55}$ are presented and the influence of temperature on the spectrum of isomers is discussed in the light of the computed caloric curves. The role of the model and the vibrational quantum effects at low temperature are shown to be significant up to room temperature. In particular, the choice of the model strongly affects the thermal behavior and the melting temperature. Finally, some concluding remarks are given in "Conclusions".

## METHODS

### *Tight-Binding Hamiltonian and EAM Model*

The binding energy of lithium clusters is modeled using a version of the quantum tight-binding (TB) Hamiltonian previously developed for sodium clusters[58], and further adapted for silver clusters[59]. We do not give the full

details of the TB model here, these are contained in ref.[58] Using the notations of this paper, a difference with the model for sodium is that the distance-dependent hopping integrals $t_{ss}(r)$ and $t_{sz}(r)$ are both taken as $t(r) = Ar^p \exp(-ar)$. The diagonal interaction $\rho(r)$ accounts for the short-range repulsion as well as an effective long-range dispersion attraction:

$$\rho(r) = B \exp(-br) - f_{cut}(r) \frac{C}{r^{\nu}} \qquad (1)$$

with a cut-off function $f_{cut}$ taken as an Aziz form[60] with a cut-off radius $d$.

All parameters were numerically obtained by fitting the potential curves of the two lowest electronic states of $Li_2$ and the dissociation energy of $Li_4$, as obtained from reference CI calculations. They are given by $A_{ss} = -1.95 \times 10^{-4}\ E_h$ and $A_{sz} = 9.1 \times 10^{-6}\ E_h$; $p_{ss} = 8$ and $p_{sz} = 10$; $a_{ss} = 1.80\ a_0^{-1}$ and $a_{sz} = 1.65\ a_0^{-1}$ for the hopping integrals, and by $B = 2.406\ E_h$, $b = 1.494\ a_0^{-1}$, $C = 6.587\ E_h\ a_0^6$, $\nu = 5.90$, and $d = 4.826\ a_0$ for the diagonal term.

We have also used an explicit, semi-empirical embedded-atom model potential of the Gupta type[61], the parameters being taken from the work by Li et al.[62] This EAM potential was fitted to reproduce bulk properties only, and predicts the melting point of fcc lithium to be above 500 K, in notable overestimation with respect to the experimental value (453.7 K).

*Sampling the Potential Energy Surfaces*

The stable isomers of $Li_n$ clusters have been located by periodically quenching typical configurations extracted from exchange Monte Carlo[63] simulations. More specifically, 40 trajectories were simultaneously propagated in the canonical ensemble, in the temperature range $10\ K \le T \le 600\ K$. 30 temperatures were distributed regularly in this interval, and ten replicas were added at low temperature to enhance swap moves. The swap moves themselves were carried out using the recent all-exchange strategy[64].

For global optimization purposes, the MC simulations were initiated from plausible global minima taken from sodium clusters[57], further locally optimized. For sampling purposes, $10^6$ MC steps were performed for each replica, and only the last $5 \times 10^5$ steps were included in the statistical averages. The distributions of potential energies were post-processed using a histogram reweighting procedure, hence providing the classical partition function $Z_c(T)$ and the classical heat capacity at constant volume $C_v^c(T)$ over a broad temperature range.

By repeating the quenches during the final Monte Carlo simulations, many isomers {α} were also recorded along with their relative probabilities. 1 000 quenches were periodically performed for each trajectory.

*Caloric Curves and Quantum Effects*

The caloric curves obtained from exchange Monte Carlo simulations were corrected for quantum delocalization effects using the Pitzer–Gwinn approximation[53]. In this approach the quantum partition function $Z_q(T)$ is written as

$$Z_q(T) \approx Z_c(T) \times \frac{Z_q^H(T)}{Z_c^H(T)} \tag{2}$$

in which $Z_q^H(T)$ and $Z_c^H(T)$ stand for the harmonic partition function for quantum and classical systems, respectively. These two terms and the fraction in Eq. (*2*) are evaluated for the lowest-energy minimum, whose vibrational frequencies are denoted as $\{\omega_i, i = 1, ..., 3n - 6\}$:

$$\frac{Z_q^H(T)}{Z_c^H(T)} = \prod_{i=1}^{3n-6} \frac{\sinh \hbar\omega_i / k_B T}{\hbar\omega_i / k_B T} = Z_{PG}(T). \tag{3}$$

In Eq. (*3*), $k_B$ and $\hbar$ are the Boltzmann and Planck constants, respectively. The Pitzer–Gwinn correcting factor $Z_{PG}(T)$ leads to a temperature-dependent shift in the heat capacity as

$$C_v^q(T) \cong C_v^c(T) + 2k_B T \frac{\partial^2 \ln Z_{PG}}{\partial T^2}. \tag{4}$$

Alternatively, the superposition approximation[54] can be used to calculate the quantum partition function for a fluxional $Li_n$ cluster. The idea here is to write $Z_q(T)$ as the sum over contributions from all important basins of attraction {α} on the PES, as

$$Z_q(T) \approx \sum_\alpha g_\alpha n_\alpha Z_{q,\alpha}(T). \tag{5}$$

$Z_{q,\alpha}(T)$ is the partition function of minimum α, taken here in the harmonic approximation. $n_\alpha$ is a factor accounting for the number of permutationally

equivalent isomers, given the point group of this minimum. Finally, $g_\alpha$ is a weighting term introduced to correct for the incomplete sample of isomers in the database. Except for the very small clusters, a complete enumeration of minima is not possible, the growth being roughly exponential with the number of atoms. The weights $\{g_\alpha\}$ are found in order that the probabilities of visiting the isomers at the temperature $T_0$ of a particular replica can be reproduced (more details can be found in ref.[65]). The quantum superposition method has been used previously to estimate the temperature dependence of the polarizability in metal clusters[66] and the absorption spectrum of calcium-doped argon clusters[67].

A nice feature of the quantum superposition approach is that it is in principle exact at low temperatures, contrary to path integral methods, which tend to become numerically costly. Also, it provides a direct connection between the caloric curves and the underlying energy landscape. Its limitations are twofold. Firstly, it does not easily include intrinsic basin anharmonicities, especially in the quantum case. Empirical corrections have been suggested in the literature[65,68], but they were not needed here. Secondly, it neglects tunneling effects. Rousseau and Marx showed that such effects were not important at 10 K [30], hence this approximation should be safe here as well.

## APPLICATION TO SELECTED LITHIUM CLUSTERS

The three cluster sizes chosen in the present work have previously received attention from several groups[17,22,23,27,30,31,35,39] thus they provide a natural ground for comparison between different models and/or different methods.

### $Li_8$

We start by illustrating in Figs 1 and 2 the entire set of stable structures found for $Li_8$ using the TB Hamiltonian and the EAM model, respectively. In the case of the quantum TB model, the $T_d$ fully capped tetrahedron (or hypertetrahedron) is the global minimum, in agreement with most *ab initio* calculations[17,18,25,39], but also with Raman spectroscopy experiments[17]. The vibrational frequencies obtained with the TB model (the eight modes are found at 93, 151, 217, 240, 246, 276, 335 and 337 $cm^{-1}$, respectively) also compare well with the matrix-isolated study of ref.[17] The second energy minimum, namely the $D_{2d}$ doubly capped square bipyramid, lies only 0.02 eV above the ground state minimum. The third important isomer is the capped pentagonal bipyramid, 0.13 eV above the global minimum. Inter-

estingly, several open structures are found as stable minima, at least 0.4 eV above isomer a. In particular, they include a fully planar $C_{2v}$ minimum and two isomers with a single tail atom. More minima are likely to exist for the present TB model. The inclusion of zero-point energy does not alter the ordering between isomers in Fig. 1, in agreement with the work by Gardet and coworkers[25] and by Rousseau and Marx[28].

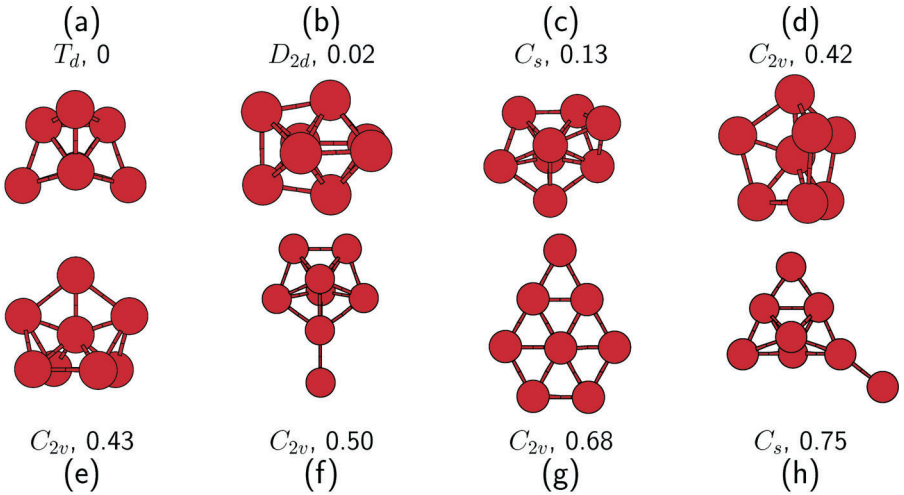


FIG. 1
Low-energy structures of $Li_8$ obtained with the quantum TB Hamiltonian. The point groups and the energies (in eV) relative to the global minimum $T_d$ structure are indicated. The energies include the zero-point contribution at the harmonic level

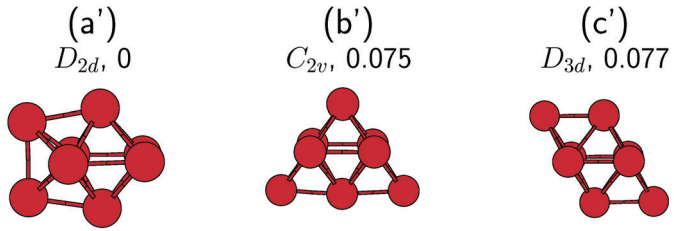


FIG. 2
Low-energy structures of $Li_8$ obtained with the empirical EAM model. The point groups and the energies (in eV) relative to the global minimum $D_{2d}$ structure are indicated. The energies include the zero-point contribution at the harmonic level

There are only three minima found for the EAM potential. All of them are based on the square bipyramid, with two capping atoms at different locations. The global minimum is identical to the second isomer of the TB model, apart from local geometry distortions. It is also worth noting that the three minima lie in a rather narrow energy range, and that their ordering is also preserved after including the zero-point correction. The vibrational frequencies of the ground state isomer notably differ from the TB values: the 14 modes all lie in the 48–163 $cm^{-1}$ range.

The strong differences exhibited by the two models reflect their distinct nature, the TB model being more explicitly quantum, while the EAM is closer to orbital-free semiclassical descriptions[57]. The situation is thus very similar to that in sodium clusters[57,58].

The finite temperature populations of isomers in the TB model have been estimated by quenching the trajectories of exchange Monte Carlo simulations. More than 99% of the quenches ended in isomers a, b, or c, and the relative proportions of the remaining isomers could not be estimated with great accuracy. The weights of the isomers can also be estimated from the harmonic superposition approximation, using the vibrational frequencies, energies and point groups of each isomer. These two methods are compared in Fig. 3. They show a similar pattern, the two methods being in semiquantitative agreement: isomer b gets more and more visited, hitting maximum probability near room temperature, and isomer c becomes dominant

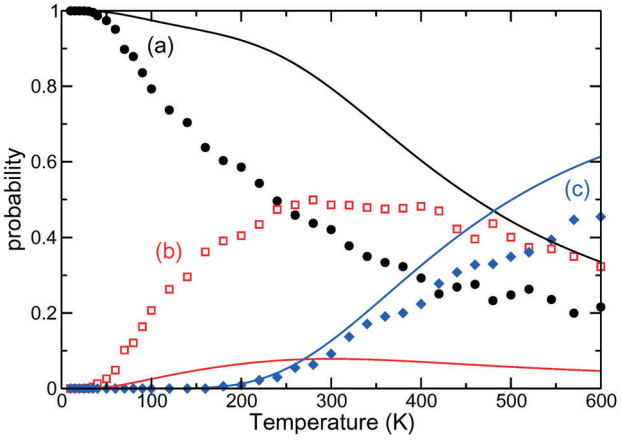


FIG. 3
Probability of finding isomers a, b, or c in the TB model as a function of temperature. The symbols are the results of 1 000 quenches from exchange Monte Carlo trajectories, and the continuous lines are obtained using the harmonic superposition approximation

at 450–500 K. The superposition approximation somewhat underestimates the weight of the $D_{2d}$ minimum. A similar calculation performed with the EAM model (data not shown here) surprisingly shows the opposite results, namely the quenches lead to the $D_{2d}$ isomer more than 90% of the time in the whole range 0–600 K. The disagreement between quenching and the superposition approximation emphasizes the anharmonicities of the potential energy landscape, especially near the EAM $D_{2d}$ minimum. The caloric curves obtained for $Li_8$ do not show any major sign of isomerization, the size being probably too small for any clear peak to be seen in the heat capacity.

### $Li_{20}$

According to our TB model, the global minimum of $Li_{20}$ is a $C_3$ capped icosahedron, similar to the lowest energy isomer of $Na_{20}$ in refs[58], and in agreement with the study by Fournier and coworkers[39]. The EAM potential predicts a capped double icosahedron as the most stable structure. This isomer is close, bot not identical, to the geometry found by Rousseau and Marx[30,31] using density functional theory.

Exchange Monte Carlo simulations of $Li_{20}$ and the subsequent quenching of configurations eventually lead to 415 distinct isomers in the TB case, but only 58 for the EAM potential. The canonical heat capacities obtained using either the Pitzer–Gwinn approximation or the quantum harmonic superposition method are presented in Fig. 4 for the two models. In these figures,

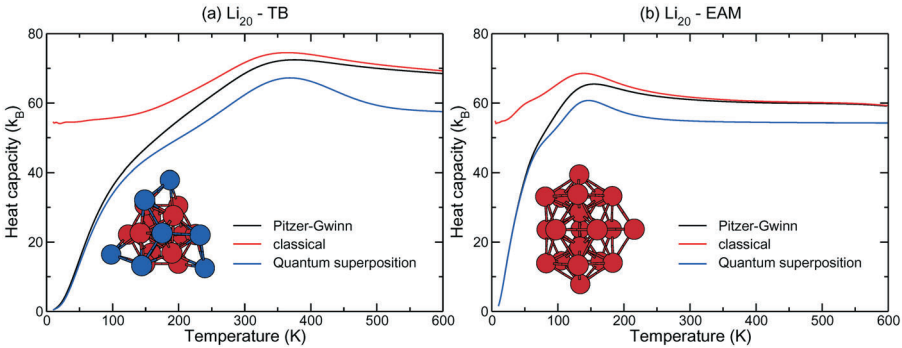


FIG. 4

Heat capacity of $Li_{20}$ obtained from exchange Monte Carlo simulations (red lines), quantum corrected using the Pitzer–Gwinn approximation (black lines), or from the quantum harmonic superposition approximation (blue lines). (a) TB model; (b) EAM model. The global minimum structures are also represented in the corresponding panel. In the TB case, the blue atoms are located on the top of a core icosahedron (red atoms)

the structures of the global minima are shown as well, and the classical heat capacities are given as references. The tight-binding Hamiltonian leads to a single broad peak in the heat capacity near 350 K. When quantum effects are included, this peak does not significantly vary; mostly the low-temperature behavior is affected. Vibrational anharmonicities can be seen from the deviations of the classical heat capacities with the Dulong–Petit limit[68], under the form of a positive slope. This explains why the PG curve, which partially accounts for the intrinsic basin anharmonicities, is located above the quantum superposition result. Still the two methods agree quite well.

The EAM potential leads to a main broad peak in the classical heat capacity near 120 K, but also a clear shoulder at 40 K. The melting temperature, inferred from the top of the main peak, is therefore much lower for the EAM model. The same is true for the latent heats, as estimated by the area below the peak. When delocalization effects are taken into account, the premelting shoulder is entirely washed out, and the two quantum curves again differ due to vibrational anharmonicities. The similarity between the present curves and the results for $Na_{20}$ using a similar EAM model[48] indicate that the two alkali cluster undergo similar finite temperature variations. Coexistence of several isomers of $Li_{20}$ below 100 K is possible, but is contradicted by the study by Rousseau and Marx[30], who found the

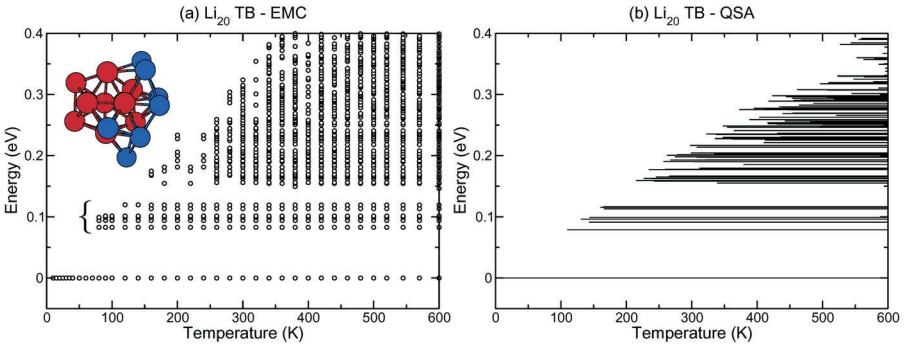


FIG. 5

Spectra of isomers of $Li_{20}$ in the TB model. (a) Classical spectrum obtained from periodically quenching the exchange Monte Carlo trajectories (1 000 times per trajectory). (b) Spectrum obtained from the quantum superposition approximation, an isomer being present if its relative weight exceeds $10^{-3}$. The energies are given relative to the global minimum energy, with (b) or without (a) zero-point correction. In panel (a), a typical isomer of the set indicated by a curved brace is represented

root-mean-square bond length fluctuation index δ to remain around 5% at 100 K in the classical case.

Therefore the TB model seems more realistic for describing $Li_{20}$. The spectrum of isomers obtained from quenching the classical TB trajectories is represented in Fig. 5a. In this figure, each isomer appearing at least once among the 1 000 quenches is represented as a symbol, for all temperatures in the simulation. We have constructed a quantum spectrum along the same ideas, by calculating the relative probabilities $\{p_\alpha(T)\}$ of all isomers as a function of temperature, using the quantum superposition approach. Isomers are then represented if their probability equals or exceeds $10^{-3}$. This continuous spectrum is represented in Fig. 5b. The general shape of the two spectra is the same. A set of intermediate minima located near 0.1 eV above the global minimum appears at temperatures near 150 K, and the remaining isomers lying more than 0.15 eV above the global minimum gradually appear at temperatures higher than 200 K. The isomers of the intermediate set are few (8 were found) and all based on the same icosahedral motif capped by 7 atoms. In Fig. 5a we have represented such a typical isomer. The two clear energy gaps, which separate this set of minima from both the ground state and the remaining isomers suggest that these intermediate minima form a well defined thermodynamical phase, in which the icosahedral core is partially wetted. This situation was observed in $Na_{20}$ described by a similar TB model[69]. However, and contrary to the results of ref.[69], we find no evidence here for any effect of this surface melting phenomenon on the caloric curve of $Li_{20}$.

### $Li_{55}$

The structure of $Li_{55}$ was investigated by Sung et al.[20] at first-principle levels. These authors were not able to locate better candidates than the two-layer Mackay icosahedron. While the putative global minima obtained here are both based on the icosahedron for both TB and EAM, significant Jahn–Teller distortions are found for the TB Hamiltonian. The heat capacity curves are presented in Fig. 6, and the spectra of isomers calculated by periodic quenching are shown in Fig. 7. The global minima, also depicted in Fig. 7 for the two models, illustrate the distortion in the TB structure, which exhibits a marked convex character and ends in the $S_6$ point group (instead of $I_h$ for the EAM potential). The classical heat capacities are mainly unimodal for the two models, but the melting peaks are located at very different temperatures, 350 K (TB) or about 100 K (EAM). The latent heats also significantly differ, from 24.2 meV/atom for the TB model to

12.8 meV/atom for the empirical potential. Including vibrational delocalization effects, the melting peak does not vary much with respect to the classical curves, and the Pitzer–Gwinn and quantum harmonic superposition results agree reasonably with each other.

The spectra of isomers in Fig. 7 both show that melting correlates with the appearance of many isomers separated from the global minimum by an energy gap. This gap is about 0.2 eV in the TB model, but only 0.1 eV in the EAM model. More generally, the spectra themselves are similar within a

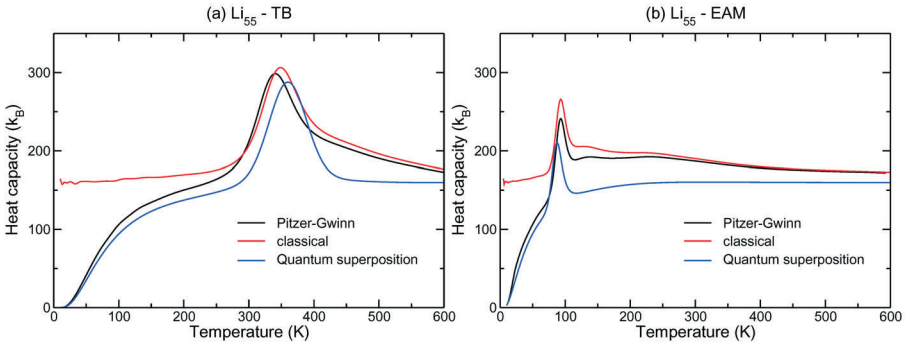


FIG. 6

Heat capacity of $Li_{55}$ obtained from exchange Monte Carlo simulations (red lines), quantum corrected using the Pitzer–Gwinn approximation (black lines), or from the quantum harmonic superposition approximation (blue lines). (a) TB model; (b) EAM model

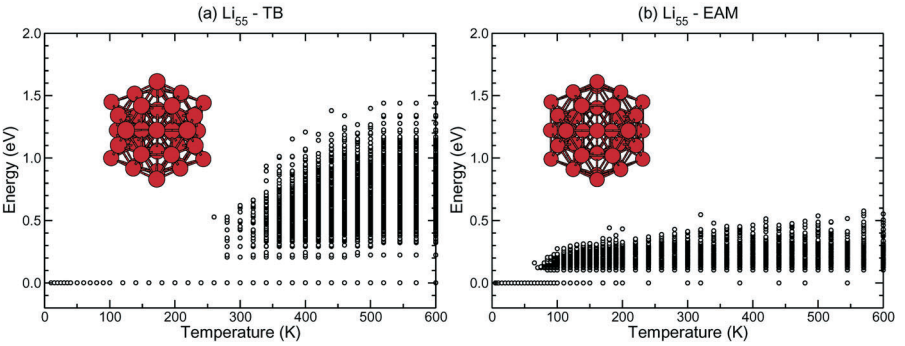


FIG. 7

Classical spectrum of isomers of $Li_{55}$ described by (a) the TB model; (b) the EAM model. Both spectra have been obtained from periodically quenching the exchange Monte Carlo trajectories (1 000 times per trajectory). The icosahedral-based global minimum corresponding to each model is indicated in both panels

scaling factor of ~2–3, consistently with the factor in the latent heats. The reduced gap in the EAM potential obviously matches the reduced melting temperature, the other factors responsible for the discrepancy with the TB results being probably changes in the vibrational frequencies. The Jahn–Teller distortions may play an unexpected role in thermodynamics, affecting the different statistical weights of the global minimum: as a perfect icosahedron, $n_\alpha = 1/120$, but in the $S_6$ symmetry $n_\alpha = 1/12$.

*Discussion*

The above investigation has shown that the tight-binding Hamiltonian and the empirical embedded-atom model lead to common features in the caloric curves of lithium clusters, namely a two-step melting process in $Li_{20}$ and a single, first-order-like process in $Li_{55}$. However, there are several significant differences between these models. The first is qualitative: while premelting effects are seen on the classical caloric curve of EAM $Li_{20}$, none are found with the TB model. Most notably, the models differ quantitatively, the melting temperatures being around 350–400 K for TB and only 100–150 K for EAM. Similar trends were found previously for sodium[48]. The systematic overestimation (or underestimation) of the melting temperature with respect to the experimental value was interpreted as the result of the parametrization of the corresponding model, lacking any bulk (respectively molecular) property in the TB (respectively EAM) case. The present empirical potential surprisingly predicts a particularly low melting point for $Li_{55}$, even lower than for $Li_{20}$. The *ab initio* study by Rousseau and Marx[30,31] is in disagreement with this result, but is compatible with the caloric curves obtained with the TB model.

Quantum delocalization effects seem to have a limited influence on the caloric curves. Contrary to some rare-gas clusters such as $Ne_{38}$ [65], the zero-point corrections do not qualitatively alter the stable phases or the heat capacities, except in the low-temperature Debye regime. Nor do they lead to an appreciable decrease in the melting point with respect to the classical value, as is for instance the case in $Ne_{13}$ [65]. It is not excluded that quantum effects could play a larger role, especially for clusters with a polyicosahedral ground state structure[20] often associated with lower vibrational frequencies[65]. To some extent, and in a way similar to entropic stabilization, zero-point effect could also stabilize the liquid state relatively to the ground state structure, hence decreasing the chance of observing a possible backbending in the microcanonical caloric curve.

Our results shed doubts about the ability of the present EAM potential and its current parameters to describe properly metallic bonding in lithium clusters, and to reproduce some finite size effects. The strong underestimation of the melting point is clearly associated with several outcomes of this model, including the relatively low binding energies and vibrational frequencies. It would certainly be useful to perform a new parametrization by incorporating a proper fitting of the bulk melting point (presently – and surprisingly – overestimated by more than 100 K [62]), as well as some small-scale properties. However, the polytetrahedral structure of $Li_8$ and $Li_{20}$ will be difficult to reproduce with a soft potential such as the current EAM with exponential decay functions. More complicated forms for the embedding energy could be devised, using for instance a force matching procedure based on simulations performed at higher levels of theory.

## CONCLUSIONS

Small lithium clusters melt in a way very similar to other alkali clusters. In this work, we have used two atomistic models to calculate the canonical caloric curves of selected $Li_n$ clusters with $n$ = 8, 20, and 55 atoms. Our first model is a distance-dependent tight-binding Hamiltonian, with parameters chosen to reproduce molecular properties. This TB model correctly predicts the hypertetrahedral isomer to be the most stable for $Li_8$, in agreement with most electronic structure calculations. We have also used an empirical embedded-atom model, with parameters taken from ref.[62] and chosen to reproduce bulk properties only. The EAM potential leads to structures that are essentially identical to those of rare-gas clusters.

The finite temperature behavior was studied using a combination of Monte Carlo simulations improved with the all-exchange strategy[63,64]. Periodic quenching of the replica configurations was carried out in order to relate the results to the underlying features of the energy landscape. Incidentally, the set of minima obtained from systematic quenching allowed us to construct the caloric curves via a harmonic superposition approximation[65]. As emphasized by Rousseau and Marx[30,31], vibrational delocalization effects can be important for a light element such as lithium. The Pitzer–Gwinn approximation[53] was used here to correct the classical heat capacity at low temperatures. In the superposition approach, the incorporation of delocalization effects is straightforward through explicit forms for the quantum harmonic partition functions.

We have generally found that $Li_{20}$ melts through an intermediate, premelting state, this state being seen on the caloric curves only in the

EAM case. The TB model leads to a surface melting phenomenon similar to the one found in $Na_{20}$ [69], but revisited here in the light of the isomers. Contrary to the 20-atom cluster, $Li_{55}$ exhibits a more conventional singler-step melting process in both models.

Delocalization effects were seen to wash out premelting effects from the heat capacity of EAM $Li_{20}$, but no significant shift in the melting point was identified. The PG and superposition methods give results in very satisfactory agreement with each other.

The melting points with the TB model were found to be in the range of 350–400 K, but only 100–150 K for the EAM potential. Comparing with the *ab initio* molecular dynamics results of Rousseau and Marx[30,31], who found $Li_{20}$ to be clearly rigid at 100 K in the classical case ($\delta < 5\%$), only the TB model seems reasonably close to these findings.

We have focused here on the equilibrium thermodynamics of neutral lithium clusters; other aspects could be investigated as well. The isomerization dynamics, for instance, could be explicitly simulated using classical molecular dynamics, along the lines of the work by Jellinek and Bonačić-Koutecký[22,23,27]. The kinetics of isomerization could also be addressed, using master equation techniques[70] or kinetic Monte Carlo. Finally, the TB model is not limited to neutral species, and cationic clusters could be studied similarly. This will be particularly important for future experiments aiming at measuring caloric curves on size-selected clusters.

## REFERENCES


1. Knight W. D., Clemenger K. L., De Heer W. A., Saunders W. A.: *Phys. Rev. Lett.* **1985**, *52*, 2141.
2. a) Beck D. E.: *Solid State Commmun.* **1984**, *49*, 381; b) Ekardt W.: *Phys. Rev. B* **1984**, *29*, 1558; c) Brack M.: *Rev. Mod. Phys.* **1993**, *65*, 677; d) de Heer W.: *Rev. Mod. Phys.* **1993**, *65*, 611; e) Martin T. P., Bergman T., Gölich H., Lange T.: *Chem. Phys. Lett.* **1990**, *172*, 209.
3. a) Balian R., Bloch C.: *Ann. Phys.* **1972**, *69*, 76; b) Nishioka H., Hansen K., Mottelson B. R.: *Phys. Rev. B* **1990**, *42*, 9377; c) Pedersen J., Bjornholm S., Borgreen J., Hansen K., Martin T. P., Rassmussen H. D.: *Nature* **1991**, *353*, 733; d) Pellarin M., Baguenard B., Bordas C., Broyer C., Lermé M., Vilalle J.-L.: *Phys. Rev. B* **1993**, *48*, 17645.
4. a) Nilsson S. G.: *Mat. Fys. Medd. K. Dan Vidensk. Selsk* **1955**, *29*, No. 16; b) Ekardt W., Penzar Z.: *Phys. Rev. B* **1991**, *43*, 1322; c) Montag B., Reinhardt P. G.: *Z. Phys. D* **1995**, *33*, 265; d) Yannouleas C., Landman U.: *Phys. Rev. Lett.* **1997**, *78*, 1424; e) Kümmel S., Brack M., Reinhardt P. G.: *Phys. Rev. B* **2000**, *62*, 7602.
5. Koutecký J., Fantucci P.: *Chem. Rev.* **1986**, *86*, 539.
6. Fantucci P., Bonačić-Koutecký V., Koutecký J. in: *Elemental and Molecular Clusters* (G. Benedek, T. P. Martin and G. Pacchioni, Eds). Springer Ser. in *Mater. Sci.* **1987**, *6*.

7. Koutecký J., Bonačić-Koutecký V., Boustani I., Fantucci P., Pewerstorf W. in: *Large Finite Systems* (J. Jortner, A. Pullman and B. Pullman, Eds), p. 303. Reidel, Dordrecht 1987.
8. Bonačić-Koutecký V., Fantucci P., Koutecký J.: *Chem. Rev.* **1991**, *91*, 1035.
9. Bonačić-Koutecký V., Fantucci P., Koutecký J. in: *Clusters of Atoms and Molecules* (H. A. Haberland, Ed.). Springer Ser. in *Chem. Phys.* **1994**, *52*, 15.
10. Bonačić-Koutecký V., Fantucci P., Koutecký J.: *Comments At. Mol. Phys.: Nuclear Aspects of Simple Metal Clusters*. Gordon, Breach Science Publishers, vol. 31, New York 1995.
11. Moyano G. E., Wesendrup R., Söhnel T., Schwerdtfeger P.: *Phys. Rev. Lett.* **2002**, *89*, 103401.
12. a) Breaux G. A., Benirschke R. C., Sugai T., Kinnear B. S., Jarrold M. F.: *Phys. Rev. Lett.* **2003**, *91*, 215508; b) Chacko S., Joshi K., Kanhere D. G., Blundell S. A.: *Phys. Rev. Lett.* **2004**, *92*, 135506.
13. a) Shvartsburg A. A., Jarrold M. F.: *Phys. Rev. Lett.* **2000**, *85*, 2530; b) Joshi K., Kanhere D. G., Blundell S. A.: *Phys. Rev. B* **2003**, *67*, 235413; c) Majumder C., Kumar V., Mizuseki H., Kawazoe Y.: *Phys. Rev. B* **2001**, *64*, 233405.
14. Dugourd Ph., Rayane D., Labastie P., Vezin B., Chevaleyre J., Broyer M.: *Chem. Phys. Lett.* **1992**, *197*, 433.
15. Benichou E., Antoine R., Rayane D., Vezin B., Dalby F. W., Dugourd Ph., Broyer M., Ristori C., Chandezon F., Huber B. A., Rocco J. C., Blundell S. A., Guet C.: *Phys. Rev. A* **1999**, *59*, R1.
16. Ellert C., Schmidt M., Schmitt C., Haberland H.: *Phys. Rev. B* **1999**, *59*, R7841.
17. Kornath A., Kaufmann A., Zoermer A., Ludwig R.: *J. Chem. Phys.* **2003**, *118*, 6957.
18. Boustani I., Pewestorf W., Fantucci P., Bonačić-Koutecký V., Koutecký J.: *Phys. Rev. B* **1987**, *35*, 9437.
19. Koutecký J., Boustani I., Bonačić-Koutecký V.: *Int. J. Quantum Chem.* **1990**, *38*, 149.
20. Sung M.-W., Kawai R., Weare J. H.: *Phys. Rev. Lett.* **1994**, *73*, 3552.
21. Kawai R., Tombrello J. F., Weare J. H.: *Phys. Rev. A* **1994**, *49*, 4236.
22. Jellinek J., Bonačić-Koutecký V., Fantucci P., Wiechert M.: *J. Chem. Phys.* **1994**, *101*, 10092.
23. Fantucci P., Bonačić-Koutecký V., Jellinek J., Wiechert M., Harrison R. J., Guest M. F.: *Chem. Phys. Lett.* **1996**, *250*, 47.
24. Rao B. K., Jena P., Ray A. K.: *Phys. Rev. Lett.* **1996**, *76*, 2878.
25. Gardet G., Rogemond F., Chermette H.: *J. Chem. Phys.* **1996**, *105*, 9933.
26. a) Yannouleas C., Landman U.: *J. Chem. Phys.* **1997**, *107*, 1032; b) Gardet G., Rogemond R., Chermette H.: *J. Chem. Phys.* **1997**, *107*, 1034.
27. Reichardt D., Bonačić-Koutecký V., Fantucci P., Jellinek J.: *Chem. Phys. Lett.* **1997**, *279*, 129.
28. Rousseau R., Marx D.: *Phys. Rev. A* **1997**, *56*, 617.
29. Mohallem J. R., Vianna R. O., Quintão A. D., Pavão A. C., McWeeny R.: *Z. Phys. D: At., Mol. Clusters* **1997**, *42*, 135.
30. Rousseau R., Marx D.: *Phys. Rev. Lett.* **1998**, *80*, 2574.
31. Rousseau R., Marx D.: *J. Chem. Phys.* **1999**, *111*, 5091.
32. Quintão A. D., Vianna R. O., Mohallem J. R.: *Eur. Phys. J. D* **1999**, *6*, 89.
33. de Visser S. P., Alpert Y., Danovich D., Shaik S.: *J. Phys. Chem. A* **2000**, *104*, 11223.
34. Rousseau R., Marx D.: *Chem. Eur. J.* **2000**, *6*, 2982.
35. Srinivas S., Jellinek J.: *Phys. Status Solidi B* **2000**, *217*, 311.
36. Fuentealba P., Savin A.: *J. Phys. Chem. A* **2001**, *105*, 11531.

37. de Visser S. P., Danovich D., Wu W., Shaik S.: *J. Phys. Chem. A* **2002**, *106*, 4961.
38. Hotta S., Doi K., Nakamura K., Tachibana A.: *J. Chem. Phys.* **2002**, *117*, 142.
39. Fournier R., Cheng J. B. Y., Wong A.: *J. Chem. Phys.* **2003**, *119*, 9444.
40. de Visser S. P., Danovich D., Shaik S.: *Phys. Chem. Chem. Phys.* **2003**, *5*, 158.
41. Wheeler S. E., Sattelmeyer K. W., Schleyer P. v. R., Schaefer H. F., III: *J. Chem. Phys.* **2004**, *120*, 4683.
42. Lee M.-S., Gowtham S., He H., Lau K.-C., Pan L., Kanhere D. G.: *Phys. Rev. B* **2006**, *74*, 245412.
43. Chandrakumar K. R. S., Ghanty T. K., Ghosh S. K.: *J. Phys. Chem. A* **2004**, *108*, 6661.
44. Wheeler S. E., Schaefer H. F., III: *J. Chem. Phys.* **2005**, *122*, 204328.
45. Chandrakumar K. R. S., Ghanty T. K., Ghosh S. K.: *Int. J. Quantum Chem.* **2005**, *105*, 166.
46. Alexandrova A. N., Boldyrev A. I.: *J. Chem. Theory Comput.* **2005**, *1*, 566.
47. Schmidt M., Kusche R., von Issendorff B., Haberland H.: *Nature (London)* **1998**, *393*, 238.
48. Calvo F., Spiegelman F.: *J. Chem. Phys.* **2000**, *112*, 2888.
49. Calvo F., Spiegelman F.: *Phys. Rev. Lett.* **2002**, *89*, 266401.
50. Rytkönen A., Manninen M.: *Eur. Phys. J. D* **2003**, *23*, 351.
51. Joshi K., Kanhere D. G., Blundell S. A.: *Phys. Rev. B* **2003**, *67*, 235413.
52. Aguado A., López J. M.: *Phys. Rev. Lett.* **2005**, *94*, 233401.
53. Pitzer K. S., Gwinn W. D.: *J. Chem. Phys.* **1942**, *10*, 428.
54. Wales D. J.: *Mol. Phys.* **1993**, *78*, 151.
55. Calvo F., Doye J. P. K., Wales D. J.: *J. Chem. Phys.* **2001**, *114*, 7312.
56. Bogdan T. V., Wales D. J., Calvo F.: *J. Chem. Phys.* **2006**, *124*, 044102.
57. Calvo F., Tran S., Blundell S. A., Guet C., Spiegelmann F.: *Phys. Rev. B* **2000**, *62*, 10394.
58. a) Poteau R., Spiegelmann F.: *Phys. Rev. B* **1992**, *45*, 1878; b) Poteau R., Spiegelmann F.: *J. Chem. Phys.* **1993**, *98*, 6540.
59. Poteau R., Heully J.-L., Spiegelmann F.: *Z. Phys. D: At., Mol. Clusters* **1997**, *40*, 479.
60. Aziz R. A., Chen H. H.: *J. Chem. Phys.* **1999**, *67*, 5719.
61. Gupta R. P.: *Phys. Rev. B* **1981**, *23*, 6265.
62. Li Y., Blaisten-Barojas E., Papaconstantopoulos D. A.: *Phys. Rev. B* **1998**, *57*, 15519.
63. Geyer G. J.: in *Computing Science, Statistics*. Proceedings of the 23rd Symposium on the Interface (E. K. Keramidas, Ed.), p. 156. Interface Foundation, Fairfax Station 1991.
64. Calvo F.: *J. Chem. Phys.* **2005**, *123*, 124106.
65. Calvo F., Doye J. P. K., Wales D. J.: *J. Chem. Phys.* **2001**, *114*, 7312.
66. Calvo F., Doye J. P. K., Wales D. J.: *Chem. Phys. Lett.* **2002**, *366*, 176.
67. Calvo F., Spiegelman F., Heitz M.-C.: *J. Chem. Phys.* **2003**, *118*, 8739.
68. Calvo F., Doye J. P. K., Wales D. J.: *J. Chem. Phys.* **2001**, *115*, 9627.
69. Poteau R., Spiegelmann F., Labastie P.: *Z. Phys. D: At., Mol. Clusters* **1994**, *30*, 57.
70. Kunz R. E., Berry R. S.: *Phys. Rev. Lett.* **1995**, *74*, 3951.